EFFICIENT BUCKLING ANALYSIS OF STIFFENED COMPOSITE AIRFRAME PARTS

C. Mittelstedt
AIRBUS Deutschland GmbH
Center of Excellence Forward and Aft Fuselage – CoE FAF
Kreetslag 10, D-21129 Hamburg
Bundesrepublik Deutschland / Federal Republic of Germany

OVERVIEW

In this contribution, orthotropic composite plates under uniform uniaxial compression braced by a centrically or eccentrically placed longitudinal stiffener are considered. A closed-form analytical method for the determination of the buckling loads N_{11}^0 of such plates is presented. Furthermore, a closed-form solution for the minimum bending stiffness $EI_{\min}$ of the stiffener is presented which enables the calculation of the bending stiffness such that only local buckling of the plate occurs while the stiffener itself remains in its original position. The presented approaches are in excellent agreement with accompanying numerical calculations. Due to their closed-form analytical nature, the required computational effort is negligible which makes such approaches very suitable for preliminary design purposes, extensive parameter studies or optimization procedures.

1. INTRODUCTION

In modern aircraft structures, stiffened plates and shells consisting of laminated composite materials are integral structural parts. Since such components must usually be classified as being rather thin-walled, the stability behaviour especially with respect to buckling is a predominant design and analysis aspect. Due to the anisotropic behaviour that is an important characteristic of such laminated composite materials, the analysis of such stiffened anisotropic plates and shells requires refined approaches when compared to their isotropic counterparts.

Let us consider an orthotropic composite plate (characterized by the plate stiffness parameters D_{11}, D_{22}, D_{12} and D_{66} according to Classical Lamimate Plate Theory, see e.g. Jones [1] or Reddy [2]) under uniform compressive load N_{11}^0 (see fig. 1, upper portion). The plate has the length a, the width b and the total thickness d, and is subjected to simply supported boundary conditions at all four plate edges such that the occurring buckling modes exhibit zero values at all edges. An orthonormal coordinate system x_1, x_2, x_3 is introduced as indicated in fig. 1, upper portion. The plate is braced by an eccentrically attached stiffener which is treated as a Bernoulli-type beam element with the cross-sectional area A, the bending moment of inertia I about the x_2-axis, and the modulus of elasticity E. The stiffener is located at the transverse coordinate $x_2 = \eta b$ such that plate is subdivided into two subplates with the widths $b_1 = \eta b$ (subplate 1) and $b_2 = b(1-\eta)$ (subplate 2).

When dealing with stiffened composite plates in actual practical applications, especially in the stages of preliminary design and structural optimization, it is firstly of highest importance to be able to determine the buckling load N_{11}^0 in a fast closed-form analytical and yet reliable manner. Secondly, it is an important task to find a stiffened plate design which will exhibit a local buckling pattern wherein the stiffener remains more or less immovable and where the plate itself buckles locally (fig. 1, lower portion), rather than encountering a global buckling shape where both the plate and the stiffener buckle. This requirement necessitates the determination of the minimum bending stiffness $EI_{\min}$ of the stiffener by which a local rather than a global buckling mode is enforced.

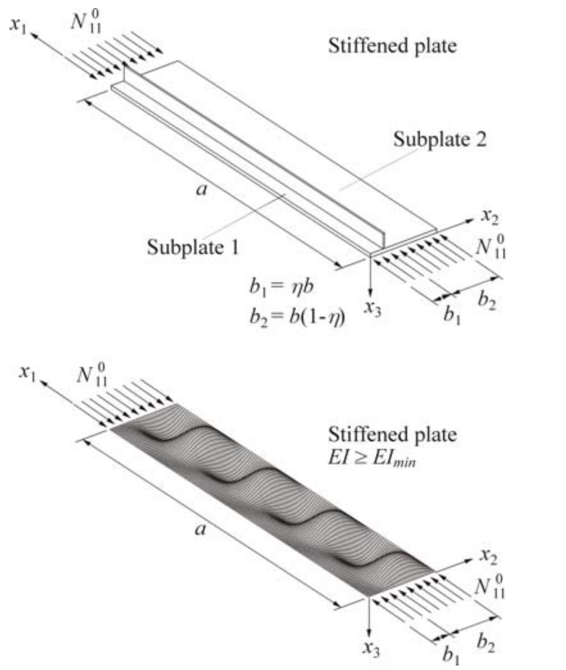

FIG 1. Structural situation (upper portion), local buckling mode when $EI \geq EI_{\min}$ (lower portion).

Naturally, when the bending stiffness EI is equal to or higher than the minimum bending stiffness $EI_{\min}$, the resultant buckling load of the stiffened plate does not depend on the properties of the stiffener but is governed by the geometry and the material properties of the plate exclusively. Furthermore, an increase of EI beyond the minimum bending stiffness $EI_{\min}$ will not lead to an increase in the buckling load of the stiffened plate since for $EI \geq EI_{\min}$ the buckling behaviour is uncoupled from the stiffener properties. These theoretical assumptions are supported by the results given in fig. 2, where the buckling loads N_{11}^0 of centrically and eccentrically stiffened stiffened composite plates with the length $a = 300$mm, the width $b = 100$mm and the laminate layups $[(0^\circ/90^\circ)_2]_S$ are given. The layer properties were set to $E_{11} = 138000$MPa, $E_{22} = 8960$MPa, $G_{12} = 7100$MPa, and $\nu_{12} = 0.30$. While the first example (fig. 2, upper portion) concerns a centrically stiffened plate (i.e. $\eta = 0.5$), the second example includes an eccentrically stiffened plate with $\eta = 0.25$. For simplicity, in both cases the stiffener has the same layup as the plate wherein a rectangular cross-section with the fixed width $b_S = 1.0$mm and a variable height h was assumed. The center of gravity was assumed to coincide with the plate middle plane.

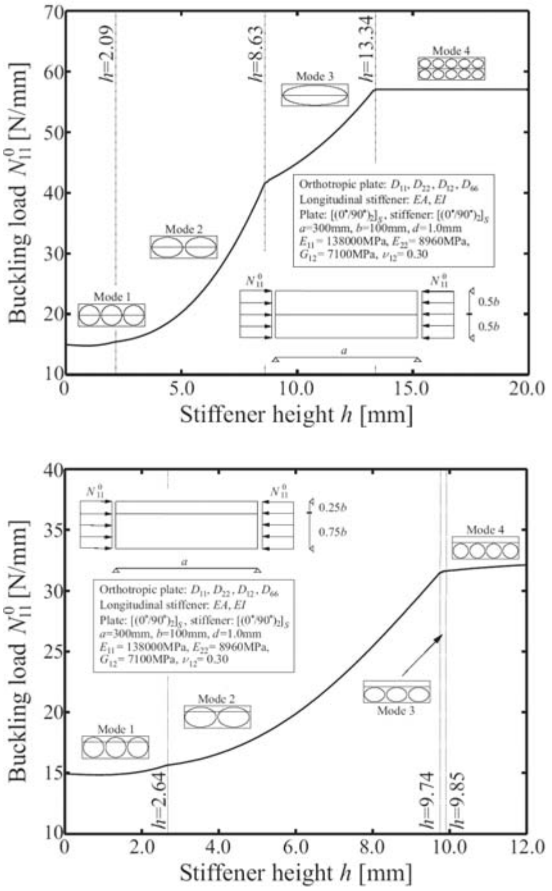

FIG 2. Buckling loads of compressively loaded composite plates with a centric stiffener ($\eta = 0.50$, upper portion) and an eccentric stiffener ($\eta = 0.25$, lower portion) for a varying height of the stiffener cross-section.

The graphs in fig. 2 were generated using the Ritz-method (see e.g. Turvey and Marshall [3] or Narita and Leissa [4]) and show the distribution of the plate buckling load N_{11}^0 as a function of the stiffener height h. The results reveal some interesting facts about the stability behaviour of stiffened composite plates.

In the case of the stiffened plate with a centric stiffener (fig. 2, upper portion), several mode changes occur when the stiffener height h is varied. While in the range $0 \le h < 2.09$mm $m = 3$ global buckling half waves are encountered, in the interval $2.09\text{mm} \le h < 8.63$mm the plate buckles globally into two half waves. A further mode change occurs in the range between $h = 8.63$mm and $h < 13.34$mm where the buckling shape exhibits one single global half wave. However, the picture changes completely when the stiffener height h is increased beyond $h = 13.34$mm where a purely local buckling mode is encountered and the plate buckles into five half waves on either side of the stiffener while the stiffener itself remains completely straight and enforces a nodal line in the buckling shape. As becomes clear from fig. 2, upper portion, for values of $h \ge 13.34$mm the buckling load N_{11}^0 remains constant and is thus uncoupled from the stiffener properties so that with $h = 13.34$mm the minimum bending stiffness $EI_{\min}$ of the stiffener can be calculated. Needless to say that an increase of h beyond $h = 13.34$mm does not lead to any benefit in the structural response with respect to buckling so that for the current example of a centrically stiffened plate we may speak of a *true minimum bending stiffness*.

In the case of the eccentrically stiffened plate (fig. 2, lower portion), analogous conclusions can be drawn. With increasing stiffener height h , a mode change from three to two global buckling half waves is encountered at $h = 2.64$mm. If a threshold value of $h = 9.74$mm is exceeded, the buckling mode switches to a local one where subplate 2 enclosed in the interval $\eta b \le x_2 \le b$ buckles into three local half waves. Interestingly enough, even though a local buckling mode is encountered for subplate 2 when $h \ge 9.74$mm, the buckling load $N_{11}^0(h)$ is not fully uncoupled from the stiffener height but shows some slight increase when h is also increased. Surprisingly, a further mode change to 4 local half waves is encountered at $h = 9.85$mm. Since the buckling load shows some slight increase also for values beyond $h = 9.74$mm, it is adequate to presently speak of a *threshold bending stiffness* rather than a true minimum stiffness beyond which a further increase of the stiffener properties is not justified by the achievable improvements in the buckling response of the stiffened plate.

The results included in fig. 2 show that the analysis of the structural behaviour of stiffened composite plates is a rather complex and challenging task. Having a reasonable estimate of the minimum bending stiffness $EI_{\min}$ is of high practical importance since in this case the buckling analysis of the stiffened plate can be reduced to a local plate buckling analysis which can often be done in a closed-form analytical manner, rather than performing an analysis of the complete stiffened plate which would necessitate more complex means of analysis, e.g. by any numerical method such as the Ritz-method or the finite element method.

From nowadays point of view, the buckling and postbuckling analysis of stiffened isotropic and laminated composite plates and shells for aircraft applications seems to be an established field of scientific investigation where a good number of sophisticated and highly efficient computational methods has been worked out since the beginning of the last century. Very early works in this field were presented by Timoshenko [5] in 1921, Way [6] in 1936, or Barbre [7] in 1939. For a selection of rather recent works see e.g. Linde et al. [8], Buermann et al. [9], Möcker and Reimerdes [10], or Wittenberg et al. [11]). However, even though a solid knowledge on the stability behaviour of stiffened aircraft parts is available, it is felt that there is still the need for efficient and accurate closed-form analysis approaches especially for composite structural parts which can be conveniently used in the stages of preliminary design where efficiency in terms of computational time and effort is a crucial factor. Furthermore, judging from the rather recent works of e.g. Bedair [12], Mijuskovic et al. [13], or Wittenberg et al. [11], the topic of the minimum stiffness of stiffeners attached to plates is still a topic of to-date research. In order to contribute to this field of investigation, in this contribution we will discuss closed-form analytical approaches to the analysis of the buckling loads N_{11}^0 of compressively loaded eccentrically stiffened composite plates as given in fig. 1, upper portion. Furthermore, a simple closed-form solution for the minimum bending stiffness $EI_{\min}$ of the stiffener will be presented. This paper is organized as follows. In section 2, the closed-form solutions for N_{11}^0 and for $EI_{\min}$ are derived. Results for the buckling behaviour of stiffened plates will be discussed in section 3. Section 4 closes the paper with a summary and some conclusions.

2. CLOSED-FORM BUCKLING ANALYSIS

The present analysis approach is based on energetic considerations for which an adequate shape function of the buckling mode has to be postulated. In order to enable a closed-form solution for both the buckling load N_{11}^0 and the minimum bending stiffness $EI_{\min}$, the displacement representation should be as simple as possible on the one hand, while on the other hand all basic characteristics of the buckling problem at hand must be captured. It is reasonable to assume that in the state of the onset of buckling, only out-of-plane deformations u_3 occur while no inplane displacements u_1 and u_2 are encountered which usually holds as long as the considered composite plates have symmetric layups such that no coupling between the inplane and the bending behaviour is active.

2.1. Buckling Analysis for *EI* < *EI*min

For a stiffened plate that is simply supported at all four edges and where $EI < EI_{\min}$, a reasonable and simple choice for the functional representation of u_3 in a variable-separable form was found to be of the following form:

(1) $$u_3(x_1, x_2) = W \sin\left(\frac{m_1 \pi x_1}{a}\right) \sin\left(\frac{\pi x_2}{b}\right).$$

Therein, it is explicitly assumed that in the longitudinal direction x_1 the stiffened plate will buckle into an a priori unknown number m_1 of half waves so that one single $\sin-$ function is sufficient for the characterization of the buckling shape, while in the transverse direction x_2 only one half wave is assumed to occur. Note that in the case of an unstiffened plate this functional representation for u_3 even describes the exact elasticity solution for the buckling behaviour under uniaxial compressive load. Further note that the functional dependence of the buckling shape has been chosen completely a priori so that the only unknown quantity in this approach is the constant W.

The potential energy Π that is stored in the stiffened plate in the buckled state can be decomposed into the following parts. Firstly, we have the potential energy Π_i^P in the plate which can be written as follows:

(2) $$\Pi_i^P = \frac{1}{2} \int_0^a \int_0^b \left(D_{11} \left(\frac{\partial^2 u_3}{\partial x_1^2} \right)^2 + D_{22} \left(\frac{\partial^2 u_3}{\partial x_2^2} \right)^2 \right) dx_2 dx_1 + \int_0^a \int_0^b \left(D_{12} \left(\frac{\partial^2 u_3}{\partial x_1^2} \right)\left(\frac{\partial^2 u_3}{\partial x_2^2} \right) + 2 D_{66} \left(\frac{\partial^2 u_3}{\partial x_1 \partial x_2} \right)^2 \right) dx_2 dx_1.$$

Secondly, the potential energy Π_i^{ST} stored in the stiffener results in:

(3) $$\Pi_i^{ST} = \frac{EI}{2} \int_0^a \left(\frac{\partial^2 u_3}{\partial x_1^2} \right)^2 |_{x_2 = \eta b}\, dx_1.$$

The contribution of the uniformly distributed inplane normal force N_{11}^0 to the elastic potential reads:

(4) $$\Pi_a^P = -\frac{N_{11}^0}{2} \int_0^a \int_0^b \left(\frac{\partial u_3}{\partial x_1} \right)^2 dx_2 dx_1.$$

Analogously, we have for the contribution of the stiffener force F:

(5) $$\Pi_a^{ST} = -\frac{F}{2} \int_0^a \left(\frac{\partial u_3}{\partial x_1} \right)^2 |_{x_2 = \eta b}\, dx_1,$$

wherein it is assumed that both the plate and the stiffener endure the same longitudinal strain so that the stiffener force F and the plate force N_{11}^0 are related by the following condition:

(6) $$F = \delta N_{11}^0 b,$$

with the auxiliary quantity δ defined as:

(7) $$\delta = \frac{EA}{E_P b d}.$$

Therein, the quantity E_P is the modulus of elasticity of the plate with respect to the x_1- direction, calculated from the laminate extensional stiffness components A_{op} (with $o, p = 1,2,6$, see Jones [1] or Reddy [2]) as:

(8) $$E_P = \frac{1}{d}\left(A_{11} - \frac{A_{12}^2}{A_{22}} \right).$$

The total potential energy Π in the elastic system in the buckled state can then be written as:

(9) $$\Pi = \Pi_i^P + \Pi_i^{ST} + \Pi_a^P + \Pi_a^{ST}.$$

The fundamental equation that governs the buckling of elastic structures requires that the first variation of the total potential energy Π in the buckled state vanishes, i.e.:

(10) $$\delta\Pi = 0.$$

Since in the present approach the only unknown quantity is the coefficient W, this condition reduces to the requirement of a vanishing first partial derivative of Π with respect to W, and we have:

(11) $$\frac{\partial \Pi}{\partial W} = 0.$$

Inserting (1) into (2), (3), (4), and (5) with (6) and executing (11), after some algebra we achieve the following closed-form expression for the buckling load N_{11}^0, provided that $EI < EI_{\min}$:

$$(12)\quad N_{11} = \frac{\pi^2 a^2}{2m_1^2\left(\frac{1}{2}+\delta\sin^2(\pi\eta)\right)}\left(\frac{m_1^4}{a^4}D_{11}+\frac{1}{b^4}D_{22}\right) + \frac{\pi^2}{b^2\left(\frac{1}{2}+\delta\sin^2(\pi\eta)\right)}\left(D_{12}+2D_{66}+\frac{m_1^2 b}{a^2}EI\sin^2(\pi\eta)\right).$$

The relevant number m_1 of buckling half waves can be determined from the stationarity requirement $\partial N_{11}^0/\partial m_1 = 0$. It is discovered that the resultant equation has only one relevant solution which reads:

$$(13)\quad m_1 = \frac{a}{b}\sqrt[4]{\frac{D_{22}}{D_{11}+\frac{2EI}{b}\sin^2(\pi\eta)}}.$$

2.2. Buckling Analysis for *EI* ≥ *EI*min

The overall structural behaviour of the stiffened plate changes significantly when the actual bending stiffness EI of the stiffener is equal to or higher than the minimum bending stiffness $EI_{\min}$ which, as was pointed out in section 1, is more adequately labelled as a threshold bending stiffness since in the case of an eccentric stiffener a true minimum bending stiffness does not exist. Provided that we have $EI \geq EI_{\min}$, the stiffener more or less remains in its original position in the state of the onset of buckling and as such enforces a nodal line in the occurring buckling shape. In this situation, subplate 2 will buckle once the critical load N_{11}^0 is exceeded while subplate 1 will offer some elastic rotational support to subplate 2. Hence, an idealization of the situation as indicated in fig. 3 is advisable where subplate 2 is modelled as a simply supported plate with additional elastic rotational restraints at the edge at $x_2 = \eta b$. The restraint stiffness is labelled as k. For convenience, an auxiliary coordinate $\bar{x}_2$ is introduced as indicated in fig. 3.

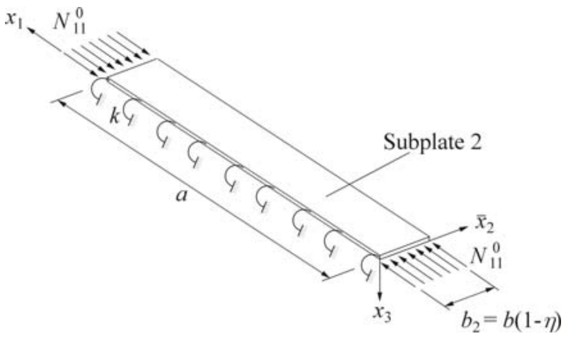

FIG 3. Idealization of the structural situation for a stiffener with $EI \geq EI_{\min}$.

For elastically restrained composite plates under compressive load, a convenient displacement shape was employed by Qiao and Shan [14] who used the following formulation for u_3:

$$(14)\quad u_3 = (x_1, \bar{x}_2) = W\sin\left(\frac{m_2\pi x_1}{a}\right)\left(\frac{\bar{x}_2}{b_2}+\psi_1\left(\frac{\bar{x}_2}{b_2}\right)^2+\psi_2\left(\frac{\bar{x}_2}{b_2}\right)^3+\psi_3\left(\frac{\bar{x}_2}{b_2}\right)^4\right).$$

Herein, it is assumed that in the longitudinal direction, one single $\sin-$function with an a priori unknown number m_2 of buckling half waves is sufficient. In the transverse direction, a polynomial of fourth order is assumed to adequately describe the buckling shape wherein the free constants ψ_1, ψ_2, ψ_3 will be adjusted to all underlying boundary conditions which can be formulated as follows. Firstly, at the loaded edges at $x_1 = 0$ and $x_1 = a$, the buckling shape has to attain zero values, i.e.:

$$(15)\quad u_3(x_1 = 0, \bar{x}_2) = u_3(x_1 = a, \bar{x}_2) = 0.$$

This condition is identically fulfilled by the $\sin-$function in the x_1-direction. Secondly, at the unloaded edges the buckling mode also has to exhibit a nodal line, hence:

$$(16)\quad u_3(x_1, \bar{x}_2 = 0) = u_3(x_1, \bar{x}_2 = b_2) = 0.$$

Thirdly, the bending moment M_{22} at the unloaded edge at $\bar{x}_2 = 0$ is proportional to the plate rotation $\partial u_3/\partial \bar{x}_2$, weighted with the restraint stiffness k:

$$(17)\quad M_{22}(x_1, \bar{x}_2 = 0) = -D_{22}\left(\frac{\partial^2 u_3}{\partial \bar{x}_2^2}\right)_{|\bar{x}_2=0} = -k\left(\frac{\partial u_3}{\partial \bar{x}_2}\right)_{|\bar{x}_2=0}.$$

Lastly, the bending moment M_{22} has to vanish at the unloaded edge at $\bar{x}_2 = b_2$:

$$(18)\quad M_{22}(x_1, \bar{x}_2 = b_2) = -D_{22}\left(\frac{\partial^2 u_3}{\partial \bar{x}_2^2}\right)_{|\bar{x}_2=b_2} = 0.$$

While the first of (16) is fulfilled identically be the employed buckling shape (14), the evaluation of the second of (16) and furthermore (17) and (18) leads to the following closed-form expressions for ψ_1, ψ_2, ψ_3:

$$(19)\quad \psi_1 = \frac{kb_2}{2D_{22}},\quad \psi_2 = -\frac{12D_{22}+5kb_2}{6D_{22}},\quad \psi_3 = \frac{3D_{22}+kb_2}{3D_{22}}.$$

In the present situation, the potential energy in the buckled state Π consists of the following portions:

$$(20)\quad \Pi = \Pi_i^P + \Pi_i^S + \Pi_a^P,$$

wherein Π_i^P is the energy stored in the plate, Π_i^S is the energy stored in the rotational springs, and Π_a^P is the contribution by the internal forces N_{11}^0. We may write:

$$(21)\quad \Pi_i^P = \frac{1}{2}\int_0^a\int_0^{b_2}\left(D_{11}\left(\frac{\partial^2 u_3}{\partial x_1^2}\right)^2 + D_{22}\left(\frac{\partial^2 u_3}{\partial \bar{x}_2^2}\right)^2\right)d\bar{x}_2 dx_1 + \int_0^a\int_0^{b_2}\left(D_{12}\left(\frac{\partial^2 u_3}{\partial x_1^2}\right)\left(\frac{\partial^2 u_3}{\partial \bar{x}_2^2}\right) + 2D_{66}\left(\frac{\partial^2 u_3}{\partial x_1 \partial \bar{x}_2}\right)^2\right)d\bar{x}_2 dx_1,$$

$$(22)\quad \Pi_i^S = \frac{k}{2}\int_0^a\left(\frac{\partial u_3}{\partial \bar{x}_2}_{|\bar{x}_2=0}\right)^2 dx_1,$$

(23) $\Pi_a^P = -\frac{N_{11}^0}{2}\int_0^a\int_0^{b_2}\left(\frac{\partial u_3}{\partial x_1}\right)^2 d\bar{x}_2 dx_1.$

Summing up the individual energy portions (21-23) as prescribed in (20), inserting the buckling shape (14) with (19) and evaluating the buckling condition (11) after some algebra leads to the following closed-form solution for the buckling load N_{11}^0:

(24) $N_{11}^0 = \frac{\beta_1}{\beta_2},$

wherein:

(25)
$$\beta_1 = \frac{D_{11}m_2^4\pi^4 b_2}{18144 D_{22}a^3}\left(1116D_{22}^2 + 285D_{22}kb_2 + 19k^2b_2^2\right) + \frac{(D_{12}+2D_{66})m_2^2\pi^2}{42D_{22}ab_2}\left(51D_{22}^2 + 13D_{22}kb_2 + k^2b_2^2\right) + \frac{a}{4b_2^3}\left(24D_{22}^2 + 11D_{22}kb_2 + k^2b_2^2\right),$$

(26) $\beta_2 = \frac{m_2^2\pi^2 b_2}{18144 D_{22}a}\left(1116D_{22}^2 + 285D_{22}kb_2 + 19k^2b_2^2\right).$

The number m_2 of buckling half waves can be determined as:

(27) $m_2 = \frac{3a\sqrt{2}}{\pi b_2}\sqrt[4]{14\frac{D_{22}}{D_{11}}\left(\frac{24D_{22}^2 + 11D_{22}kb_2 + k^2b_2^2}{1116D_{22}^2 + 285D_{22}kb_2 + 19k^2b_2^2}\right)}.$

It is important to note that the expression (24) with (25), (26) and (27) only depends on known quantities and does not require any numerical analysis and as such is of a completely closed-form analytical nature.

The restraint stiffness k can be straightforwardly determined from the principle of virtual work by taking subplate 1 as an equivalent beam with the unit width a_1 ='1' in the x_1-direction under a virtual edge bending moment $M_{22}(x_1, \bar{x}_2 = 0)$='1' (fig. 4).

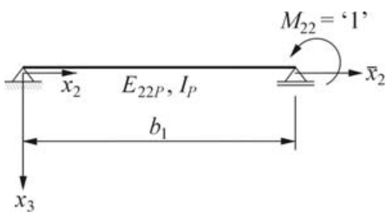

FIG 4. Idealization of subplate 1 for the determination of the elastic restraint stiffness k.

The edge rotation $\varphi(x_1, \bar{x}_2 = 0)$ can be determined as follows:

(28) $\varphi(x_1, \bar{x}_2 = 0) = \int_{-b_1}^{0}\frac{M_{22}^2(\bar{x}_2)}{E_{22P}I_P}d\bar{x}_2.$

Herein, E_{22P} is the modulus of elasticity of the plate with respect to the x_2-direction, determined from the laminate bending stiffness components D_{op} (Jones [1] or Reddy [2]) as:

(29) $E_{22P} = \frac{12}{d^3}\left(\frac{D_{11}D_{22} - D_{12}^2}{D_{11}}\right).$

The moment of inertia I_P of the plate can be calculated as:

(30) $I_P = \frac{d^3}{12}.$

The restraint stiffness k is the reciprocal value of the edge rotation φ so that we eventually have:

(31) $k = \frac{1}{\varphi} = \frac{3E_{22P}I_P}{b_1}.$

It is necessary to consider the influence of the longitudinal laminate force on subplate 1 by multiplying the restraint stiffness k with a reduction factor as follows:

(32) $k = \frac{3E_{22P}I_P}{b_1}\left(1 - \frac{N_{11,2}^0}{N_{11,1}^0}\right).$

wherein $N_{11,\alpha}^0$ (with $\alpha = 1,2$) are the critical buckling loads of subplates 1 and 2 with assumed simply supported boundary conditions. We have:

(33) $N_{11,\alpha}^0 = \frac{2\pi^2}{b_\alpha^2}\left(\sqrt{D_{11}D_{22}} + D_{12} + 2D_{66}\right).$

We eventually arrive at the following refined expression for the restraint stiffness k:

(34) $k = \frac{3E_{22P}I_P}{b_1}\left(\frac{b_2^2 - b_1^2}{b_2^2}\right).$

Note that when $b_1 = b_2$, both subplates buckle simultaneously and no restraint stiffness can be mobililzed which consequently leads to $k = 0$.

2.3. Determination of the Minimum Stiffener Bending Stiffness *EI*min

A straightforward way to determine the minimum bending stiffness of the stiffener is to assume that when the actual bending stiffness EI exactly equals the minimum bending stiffness $EI_{\min}$, two buckling modes are possible, namely on the one hand the global mode according to section 2.1, and on the other hand the local mode according to section 2.2. The minimum bending stiffness $EI_{\min}$ can then be determined from equating the two resultant expressions (12) and (24) for the buckling loads N_{11}^0 which after solving for EI eventually leads to the following representation for $EI_{\min}$:

(35)
$$EI_{\min} = \frac{b^5}{2D_{22}\pi^4}\left(\frac{1}{4\sin^2(\pi\eta)} + \delta + \delta^2\sin^2(\pi\eta)\right)\left(\frac{\varphi_1}{\varphi_2}\right)^2 - \frac{b^3}{D_{22}\pi^2}\left(\frac{1}{2}D_{12} + D_{66}\right)\left(\frac{1}{\sin^2(\pi\eta)} + 2\delta\right)\left(\frac{\varphi_1}{\varphi_2}\right) + \frac{b}{D_{22}\sin^2(\pi\eta)}\left(-\frac{1}{2}D_{11}D_{22} + \frac{1}{2}D_{12}^2 + 2D_{12}D_{66} + 2D_{66}^2\right).$$

Therein, the quantities φ_1 and φ_2 read:

(36)
$$\varphi_1 = \frac{1}{2}\left(24\frac{D_{22}^2}{b_2^2} + 11\frac{D_{22}k}{b_2} + k^2\right) + \frac{3}{7}\sqrt{14\frac{D_{22}}{D_{11}}\left(\frac{24D_{22}^2 + 11D_{22}kb_2 + k^2b_2^2}{1116D_{22}^2 + 285D_{22}kb_2 + 19k^2b_2^2}\right)} \times \left(51\frac{D_{22}}{b_2^2} + 13\frac{k}{b_2} + \frac{k^2}{D_{22}}\right)(D_{12} + 2D_{66}),$$

(37)
$$\varphi_2 = \frac{b_2^2}{1008}\sqrt{14\frac{D_{22}}{D_{11}}\left(\frac{24D_{22}^2 + 11D_{22}kb_2 + k^2b_2^2}{1116D_{22}^2 + 285D_{22}kb_2 + 19k^2b_2^2}\right)} \times \left(1116\frac{D_{22}}{b_2^2} + 285\frac{k}{b_2} + 19\frac{k^2}{D_{22}}\right).$$

Expression (35) with (36) and (37) allows for a straightforward determination of the minimum bending stiffness $EI_{\min}$ of the stiffener in a completely closed-form analytical manner. Since (35) does not depend on the plate length a, this representation for $EI_{\min}$ can be considered to be a limit case for sufficiently long stiffened composite plates. At the same time (35) provides an upper bound for $EI_{\min}$ as the results section will show and as such always delivers conservative results.

2.4. Analysis Formulation for Plates with a Centric Stiffener

If the stiffener is attached at the transverse coordinate $x_2 = \frac{b}{2}$, i.e. $\eta = 0.5$, the calculations of the buckling loads and the minimum bending stiffness simplify significantly. If the bending stiffness EI is lower than the minimum bending stiffness $EI_{\min}$, the buckling load of the plate under compression can be written in a closed-form analytical manner as:

(38)
$$N_{11}^0 = \frac{a\pi^2}{2m_1^2 b\left(\frac{1}{2} + \delta\right)}\left(D_{11}\frac{m_1^4 b}{a^3} + D_{22}\frac{a}{b^3}\right) + \frac{2\pi^2}{b\left(\frac{1}{2} + \delta\right)}\left(\frac{1}{b}\left(\frac{1}{2}D_{12} + D_{66}\right) + \frac{m_1^2}{2a^2}EI\right).$$

The number m_1 of buckling half waves reads:

(39) $$m_1 = \frac{a}{b}\sqrt[4]{\frac{D_{22}}{D_{11} + \frac{2EI}{b}}}.$$

The formulation for the minimum bending stiffness is also simplified significantly and we have:

(40) $$EI_{\min} = C_0 + C_1\delta + C_2\delta^2,$$

with:

(41)
$$C_0 = \frac{3b}{D_{22}}\left(4\sqrt{\frac{D_{22}}{D_{11}}}D_{11}(D_{12} + 2D_{66}) + \frac{5}{2}D_{11}D_{22}\right) + \frac{9b}{D_{22}}\left(\frac{1}{2}D_{12}^2 + 2D_{12}D_{66} + 2D_{66}^2\right),$$

(42)
$$C_1 = \frac{8b}{D_{22}}\left(7\sqrt{\frac{D_{22}}{D_{11}}}D_{11}(D_{12} + 2D_{66}) + 4D_{11}D_{22}\right) + \frac{24b}{D_{22}}\left(D_{12}^2 + 4D_{12}D_{66} + 4D_{66}^2\right),$$

(43)
$$C_2 = \frac{32b}{D_{22}}\left(2\sqrt{\frac{D_{22}}{D_{11}}}D_{11}(D_{12} + 2D_{66}) + D_{11}D_{22}\right) + \frac{32b}{D_{22}}\left(D_{12}^2 + 4D_{12}D_{66} + 4D_{66}^2\right).$$

The special case of an unstiffened composite plate is achieved when letting $EI \to 0$ and $\delta \to 0$ which leads to:

(44) $$N_{11}^0 = \pi^2\left(\frac{m_1^2}{a^2}D_{11} + \frac{a^2}{m_1^2 b^4}D_{22} + \frac{4}{b^2}\left(\frac{1}{2}D_{12} + D_{66}\right)\right).$$

This expression is identical to the exact solution for an orthotropic composite plate under uniform compressive load (see e.g. Reddy [2]).

In the case that the bending stiffness of the longitudinal stiffener is equal to or higher than the minimum bending stiffness $EI_{\min}$, the buckling analysis reduces to the analysis of a simply supported composite plate with only half the width b since in the case of a centric stiffener we have $b_1 = b_2$ and hence no elastic restraint is active. The buckling load in this case can be straightforwardly deduced from (44) and leads to:

(45) $$N_{11}^0 = \pi^2\left(\frac{m_2^2}{a^2}D_{11} + \frac{16a^2}{m_2^2 b^4}D_{22} + \frac{8}{b^2}(D_{12} + 2D_{66})\right).$$

For the number of buckling half waves we have:

(46) $$m_2 = \frac{2a}{b}\sqrt[4]{\frac{D_{22}}{D_{11}}}.$$

3. RESULTS AND DISCUSSION

3.1. Composite Plates

Let us discuss stiffened composite plates with the geometric and material properties as they were also employed in the introduction section. It is important to note that the expressions (35) and (40) for the minimum bending stiffness $EI_{\min}$ require an input concerning the cross-sectional area A. As a result, (35) and (40) deliver a result for $EI_{\min}$ which of course is also dependent on the cross-section of the stiffener due to the moment of inertia I. Hence, the employment of (35) and (40) obviously requires some iterative process. If we again assume a stiffener with a quadrangular cross section with $A = h \cdot 1.0$mm, we may adequately reformulate the requirement $EI \geq EI_{\min}$ as $h \geq h_{\min}$. For an assessment of $EI_{\min}$, some initial value h_0 for the stiffener height is guessed which allows for an initial estimate of the cross-sectional area A_0. The expressions (35) and (40) then lead to a first estimate $EI_{\min,1}$ of the minimum bending stiffness which in turn allows for an updated value $h_{\min,1}$. This value $h_{\min,1}$ can be used as a renewed input h_1 for an updated estimate of A_1 which leads to a refined value $EI_{\min,2}$. This process is repeated until convergence is reached such that in the $n-$th iteration step we have $EI_{\min,n-1} \cong EI_{\min,n}$, or presently $h_{\min,n-1} \cong h_{\min,n}$.

3.1.1. Plates with Centric Stiffeners

Let us firstly discuss the stability behaviour of compressively loaded composite plates with centric stiffeners, i.e. with $\eta = 0.5$. For the example plate with the layup $[(0^\circ/90^\circ)_2]_S$, the development of the solution (40) for the minimum bending stiffness $EI_{\min}$ is displayed in tab. 1 for the initial value $h_0 = 1.0$mm. Even for this rather low initial value, a rapid convergence within five iteration steps is achieved which demonstrates the robustness and simplicity of the presented analysis approach.

n	1	2	3	4	5
$h_{\min,n-1}$	1.00	11.40	13.04	13.29	13.33
$h_{\min,n}$	11.40	13.04	13.29	13.33	13.33

TAB 1. Iterative determination of the minimum stiffener height $h_{\min}$ for a composite plate with the layup $[(0^\circ/90^\circ)_2]_S$ with a centric stiffener.

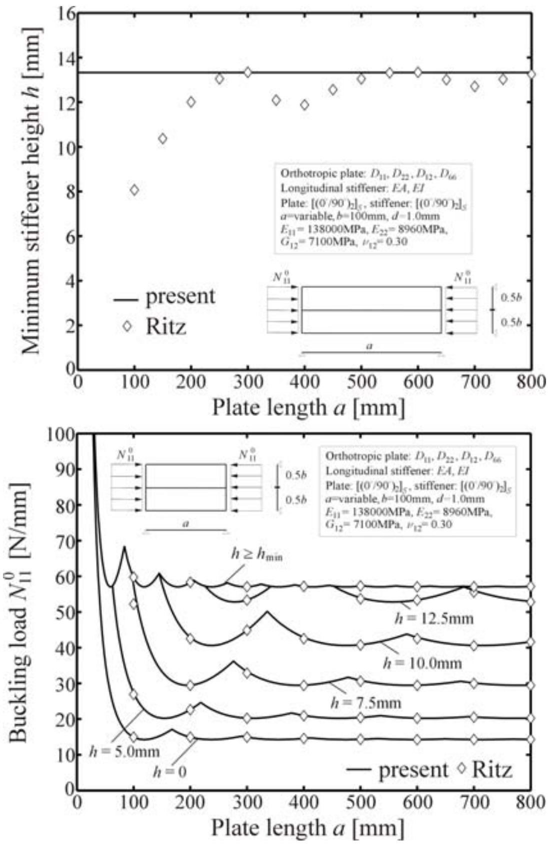

FIG 5. Comparison of the results for the minimum stiffener height $h_{\min}$ (upper portion) and for the plate buckling load N_{11}^0 (lower portion) by the present approach and the numerical approach by the Ritz-method for a composite plate with a centric stiffener and with the layup $[(0^\circ/90^\circ)_2]_S$ under compression for a variable plate length a.

In order to validate the accuracy of the present approach for both the minimum bending stiffness $EI_{\min}$ and the buckling load N_{11}^0, a comparison has been performed with a Ritz-approach employing a full double-series expansion with respect to both inplane coordinate directions x_α using classical $\sin-$ shapes for the buckling modes. Fig. 5, upper portion, shows a comparison of the results for $h_{\min}$ by both the present approach and the Ritz-method for a variable plate length a. It becomes obvious that for low aspect ratios $\frac{a}{b}$, the solution (40) for $EI_{\min}$ clearly overestimates the minimum bending stiffness by far. However, obviously the Ritz-solution approaches the present solution in an asymptotic manner for higher aspect ratios which allows for the conclusion that the solution (40) actually characterizes an upper bound for the minimum bending stiffness $EI_{\min}$ and at the same time delivers a very reliable solution for plates with a sufficiently high length a. Hence, the present analysis method for $EI_{\min}$ seemingly is a very conservative approach. It is furthermore very important to note that while the present solution (40) delivers results in a closed-form manner, the employment of the Ritz-method requires an iterative means of analysis such that for each guess of EI the buckling mode is visually inspected until the correct value for EI is found at which global buckling switches into a local buckling mode. Since one single analysis by the Ritz-method takes several seconds, depending on the degree of the employed series expansion, this is undoubtedly an arduous and time-consuming task leading to results which heavily depend on the judgement of the engineer. Such an approach is of course not suitable for practical application purposes which highlights the need e.g. for a closed-form analysis method which delivers values for $EI_{\min}$ in a reliable yet simple and straightforward manner.

A comparison between the presented closed-form solutions (38) and (45) for the buckling load N_{11}^0 and the results by the Ritz-method can be found in fig. 5, lower portion, for a variable plate length a and several values of h. Obviously, there is an excellent agreement between both approaches for all values of a and h. Note that all results curves by the present analysis method were generated within less than a second on a standard PC, while the accompanying numerical results by the Ritz-method needed about one minute to be generated. This again highlights the value of the presently derived analysis method due to its closed-form analytical nature. The results given in fig. 5, lower portion, display the buckling behaviour that is to be expected from plates under compression. While for low aspect ratios $\frac{a}{b}$ the buckling load N_{11}^0 tends towards infinite values for all h, with an increasing aspect ratio several local maxima which correspond to changes in the buckling modes occur, until an asymptotic value is approached when $\frac{a}{b} \rightarrow \infty$. Obviously, (45) indeed describes an upper bound for the buckling load of the stiffened plate since for $h \geq h_{\min}$ the buckling load is solely governed by the plate properties due to local buckling, regardless of the actual stiffener properties. As a result, at such points where the buckling curves according to (38) and (45) intersect, a discontinuous mode change between global and local buckling occurs. For the present example, such a mode change occurs for instance for $h = 7.5$mm at approximately $a = 100$mm.

3.1.2. Plates with Eccentric Stiffeners

Let us consider an orthotropic composite plate with an eccentric stiffener at $x_2 = \frac{b}{4}$ (i.e. $\eta = \frac{1}{4}$). The geometric and material data of plate and stiffener are identical to those as employed in the preceding sections. The iterative calculation of $h_{\min}$ is documented in tab. 2. As for the plates with centric stiffeners, the method converges rapidly within 5 iteration steps.

n	1	2	3	4	5
$h_{\min,n-1}$	1.00	9.16	9.78	9.82	9.83
$h_{\min,n}$	9.16	9.78	9.82	9.83	9.83

TAB 2. Iterative determination of the minimum stiffener height $h_{\min}$ for a composite plate with the layup $[(0^\circ/90^\circ)_2]_S$ with an eccentric stiffener.

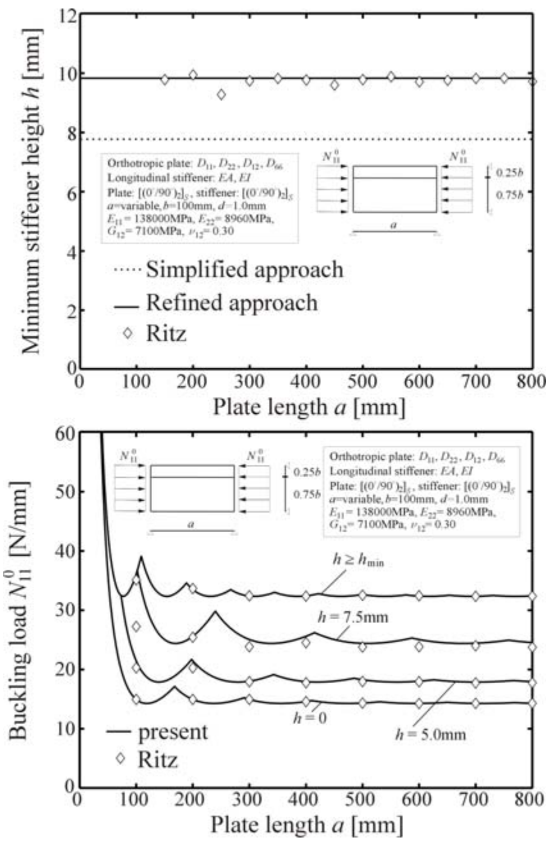

FIG 6. Comparison of the results for the minimum stiffener height $h_{\min}$ (upper portion) and for the plate buckling load N_{11}^0 (lower portion) by the present approach and the numerical approach by the Ritz-method for a composite plate with an eccentric stiffener and with the layup $[(0^\circ/90^\circ)_2]_S$ under compression for a variable plate length a.

A comparison between the present solution (35) for $EI_{\min}$ respectively $h_{\min}$ and the results by the Ritz-method can be found in fig. 6, upper portion, while the results for N_{11}^0 are compared in fig. 6, lower portion. The results labelled as *refined approach* correspond to the present solution given by (35), while the results denoted as *simplified approach* were generated assuming a simply supported subplate 2, i.e. with a vanishing restraint stiffness $k = 0$. Obviously, the present approach for eccentric stiffeners also leads to conservative results which can be interpreted as an upper bound of $EI_{\min}$. As it was the case for plates with centric stiffeners, the Ritz-method approaches the present solution in an asymptotic sense for sufficiently high aspect ratios $\frac{a}{b}$. It is an interesting outcome that the deviation between the closed-form analysis and the numerical results for lower aspect ratios $\frac{a}{b}$ is clearly not as pronounced as it was the case for plates with a centric stiffener which is a beneficial feature of the present solution (35). It is interesting to note that the assumption of a simply supported plate (simplified approach) with $k = 0$ leads to very unsatisfying and at the same time unconservative results and, even though being a first possible approach from basic engineering intuition and from the practical point of view, should not be employed for analysis purposes.

Fig. 6, lower portion, shows a comparison between the present closed-form analytical solutions (12) and (24) and the numerical results by the Ritz-method for the buckling load N_{11}^0 for several values of the stiffener height h. For all h a very satisfying agreement between both approaches is found which lends credibility to the present closed-form analysis method. Deviations between both approaches are found only for shorter plates with aspect ratios $\frac{a}{b} \leq 1.0$ for which the presently employed simple buckling shape (1) is probably not sufficient for the description of the rather complex buckling modes that occur for stout plates. Further slight deviations of the closed-form analysis equation (12) from the numerical results are found for higher values of h where seemingly the assumed symmetry of the buckling shape with respect to an imaginary longitudinal axis located at $x_2 = \frac{b}{2}$ does not deliver the complete picture of the buckling behaviour of such stiffened plates. It can be assumed that strong stiffeners lead to rather unsymmetric buckling shapes with lower amplitudes near the stiffener location so that if a higher accuracy of the results were desired, more detailed shape functions would have to be employed.

3.2. Isotropic Plates

The presented approaches for the buckling load N_{11}^0 and the minimum bending stiffness $EI_{\min}$ can also be employed for the buckling analysis of stiffened plates consisting of isotropic materials. Let us consider steel plates ($E = 210000$MPa, $\nu = 0.30$) with the same geometry properties as employed in the preceding sections for composite plates. Fig. 7 includes results for the minimum bending stiffness $EI_{\min}$ (upper portion) and the buckling load N_{11}^0 (lower portion) of a centrically stiffened plate, compared to the results according to the Ritz-method. Fig. 8 contains corresponding results for an eccentrically stiffened plate with $\eta = \frac{1}{4}$. For brevity, the iterative evaluation of the solutions for $EI_{\min}$ is not given in tabular form at this point. Needless to say, the convergence of the results is as fast as in the orthotropic case. Generally speaking, the basic characteristics of the resultant plots as given in fig. 7 and fig. 8 are the same as they were found for composite plates with centric and eccentric stiffeners so that the conclusions as they were drawn in section 3.1 in essence also hold for isotropic plates which makes a renewed discussion obsolete at this point. Nevertheless, especially the excellent accuracy on the one hand with the insignificant involved computational effort on the other hand when compared to the purely numerical approach should be mentioned which makes the presented approaches very trustworthy and efficient when dealing with actual practical applications in aircraft analysis and design, especially for preliminary design purposes or optimization procedures where one and the same analysis step has to performed dozens or even hundreds of times.

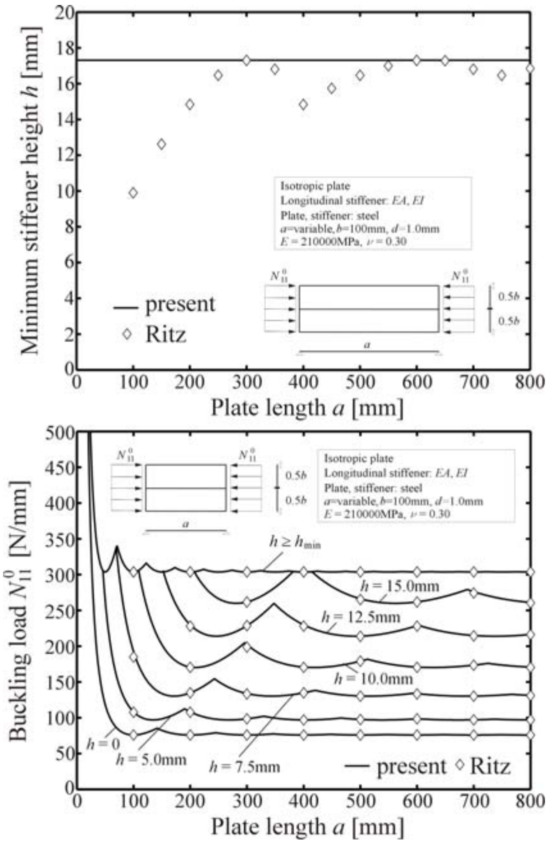

FIG 7. Comparison of the results for the minimum stiffener height $h_{\min}$ (upper portion) and for the plate buckling load N_{11}^0 (lower portion) by the present approach and the numerical approach by the Ritz-method for a steel plate with a centric stiffener under compression for a variable plate length a.

4. SUMMARY AND CONCLUSIONS

In this contribution, novel closed-form analytical solutions for the buckling loads N_{11}^0 of laminated composite plates braced by centric or eccentric longitudinal stiffeners have been presented. Furthermore, novel closed-form analytical approaches to the analysis of the required minimum bending stiffness $EI_{\min}$ of the longitudinal stiffeners such that local plate buckling occurs rather than a global buckling of both the plate and the stiffener have been derived. The presented approaches are of a completely closed-form analytical nature and do not necessitate the involvement of any numerical procedure. Hence, only a fraction of the computational time and effort that is required for corresponding numerical analysis methods has to be spent for the present closed-form analytical methods which are found to be in excellent agreement with accompanying calculations by the Ritz-method. Hence, the presented solutions can be used with confidence whenever fast and yet reliable solutions are required for the analysis of the buckling behaviour of thin-walled laminated composite and isotropic stiffened plates under compression.

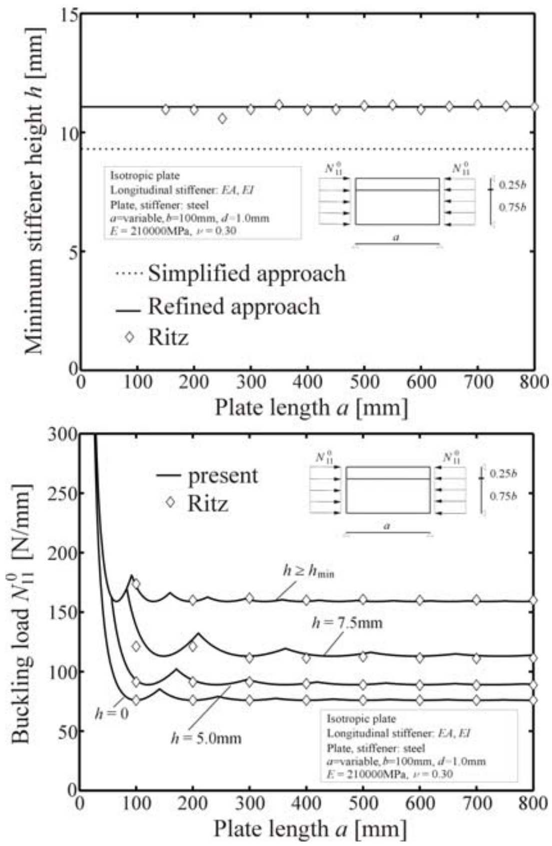

FIG 8. Comparison of the results for the minimum stiffener height $h_{\min}$ (upper portion) and for the plate buckling load N_{11}^0 (lower portion) by the present approach and the numerical approach by the Ritz-method for a steel plate with an eccentric stiffener under compression for a variable plate length a.

References

[1] Jones RM (1975). *Mechanics of composite materials*, Scripta Book Co., Washington.
[2] Reddy JN (2004). *Mechanics of laminated composite plates and shells*, second edition, CRC Press, Boca Raton et al.
[3] Turvey GJ and Marshall IH (1995). *Buckling and postbuckling of composite plates*, Chapman and Hall, London.
[4] Narita Y and Leissa AW (1990). *Buckling studies for simply supported symmetrically laminated rectangular plates*, International Journal of Mechanical Sciences 11:909-924.
[5] Timoshenko SP (1921). *Über die Stabilität versteifter Platten*, Eisenbau 12:147-163.
[6] Way S (1936). *Stability of rectangular plates under*

shear and bending forces, Journal of Applied Mechanics 3:A131-A135.

[7] Barbre R (1939). *Stability of rectangular plates with longitudinal or transverse stiffeners under uniform compression*, NACA - National Advisory Committee for Aeronautics - Technical Memorandum No. 904, Washington.

[8] Linde P, Schulz A and Rust W (2006). *Influence of modelling and solution methods on the FE-simulation of the post-buckling behaviour of stiffened aircraft fuselage panels*, Composite Structures 73:229-236.

[9] Buermann P, Rolfes R, Tessmer J and Schagerl M (2006). *A semi-analytical model for local post-buckling analysis of stiffener-and frame-stiffened cylindrical panels*, Thin-Walled Structures 44:102-114.

[10] Möcker T and Reimerdes HG (2006). *Postbuckling simulation of curved stiffened composite panels by the use of strip elements*, Composite Structures 73:237-243.

[11] Wittenberg TC, Hol JMAM and van Baten TJ (2006). *Shear buckling of flat orthotropic stiffened panels with application to glare material*, AIAA Journal 44:2179-2188.

[12] Bedair OK (1997). *The elastic behaviour of multi-stiffened plates under uniform compression*, Thin-Walled Structures 27:311-335.

[13] Mijuskovic O, Coric B and Pavlovic MN (1999). *Transverse-stiffener requirements for the post-buckling behaviour of a plate in shear*, Thin-Walled Structures 34:43-63.

[14] Qiao P and Shan L (2005). *Explicit local buckling analysis and design of fiber-reinforced plastic composite structural shapes*, Composite Structures 70:468-483.